

Experimental investigation of cracking and deformations of concrete ties reinforced with multiple bars



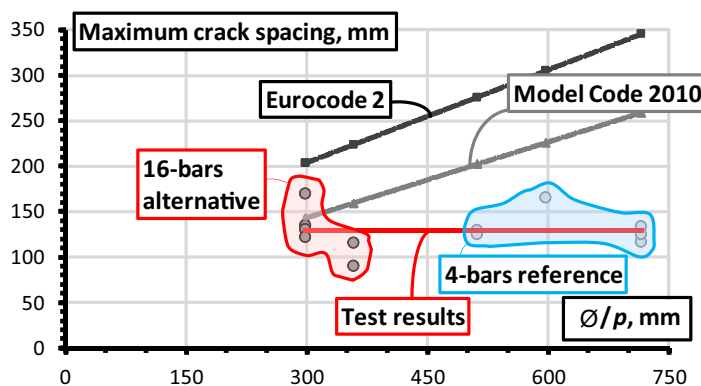
Arvydas Rimkus, Viktor Gribniak*

Research Laboratory of Innovative Building Structures, Vilnius Gediminas Technical University, Vilnius, Lithuania

HIGHLIGHTS

- Cracking and deformations of concrete ties with multiple bars are investigated.
- A specific equipment for producing and testing such ties was developed.
- Two reinforcement schemes are considered: 4-bars reference and 16-bars alternative.
- The alternative schemes secure indistinguishable deformation behaviour of identical ties.
- The experimental crack spacing is practically independent on the \varnothing/p ratio.

GRAPHICAL ABSTRACT



ARTICLE INFO

Article history:

Received 9 January 2017
 Received in revised form 21 April 2017
 Accepted 5 May 2017
 Available online 11 May 2017

Keywords:

Reinforced concrete
 Multiple bars
 Tensile test
 Deformations
 Cracking

ABSTRACT

Interpretation of test results may be inadequate even for simple test layouts. On the one hand, conventional tests, that investigate a concrete prism reinforced with a single bar in the centre, do not allow to account for the effect of variation of the diameter-to-reinforcement ratio (\varnothing/p). This important limitation should be related to the use of simple specimens in constitutive modelling. On the other hand, a tie-test typically provides measurements of average deformations of the internal reinforcing bar and the concrete surface. The experimental evidence, however, often contradicts the general assumption of the equivalence of the mean strains of reinforcement and concrete. The strain difference is closely related to the width of the concrete cover. This paper investigates the effect of distribution of bar reinforcement on deformation and cracking behaviour of tensile elements. Special testing equipment has been developed to investigate ties reinforced with multiple bars. The test program consists of 23 ties. The number and diameter of the bars vary from 4 to 16 and from 5 mm to 14 mm, respectively. Two different covers (30 mm and 50 mm) are considered as well. The deformation analysis is based on measurements of the average reinforcement and concrete surface strains. The development of cracks was investigated using digital image correlation (DIC). The Model Code 2010 and Eurocode 2 predictions are compared with the experimental data. While the Design Codes predict that the maximum crack spacing is dependent on the \varnothing/p ratio, the test results indicate that the crack distances are actually much less dependent on the reinforcement characteristics.

© 2017 Elsevier Ltd. All rights reserved.

* Corresponding author at: Head of Research Laboratory of Innovative Building Structures, Vilnius Gediminas Technical University, Sauletekio av. 11, Vilnius LT-10223, Lithuania.

E-mail address: Viktor.Gribniak@vgtu.lt (V. Gribniak).

1. Introduction

Excessive cracking due to the tensile stresses in the concrete can be identified as a key source of deterioration of reinforced concrete structures. Rostásy et al. [1], Hwang and Rizkalla [2], Williams [3], and Purainer [4] have demonstrated experimentally that distributing the same reinforcement area in a higher number of bars (of a smaller diameter) may noticeably increase the stiffness of concrete ties. Such an increase might be a consequence of two effects. On the one hand, an increase in the total bond area also increases the bond capacity to release the extra fracture energy during the crack formation stage. On the other hand, the confinement of the intact concrete between the closely spaced bars constrains the internal cracks. The test data reported by Broms and Lutz [5] supports the latter inference. Otsuka and Ozaka [6] found that the bond stiffness will increase if the distance between the reinforcement bars is reduced. Experimental results obtained by the authors [7–9] and other researchers, e.g., [5,10,11], indicated that the cracking pattern is dependent on the geometry of the specimen and the arrangement of the reinforcement. Using the test results of ties with different reinforcement and testing layouts, Rimkus et al. [12] revealed that differences in the crack spacing are dependent on the concrete cover. The total area of the bonded surface of the reinforcement with different number of bars was identified as another source of the different crack distributions.

Although a standard test setup for reinforced concrete elements under tension does not exist, the direct tensile test of a concrete prism reinforced with a single bar is the most widely used experimental layout for investigation of cracking problems [13]. Despite the apparent simplicity of the setup, the interpretation of the test results might be misleading: the experimental evidence often disagrees with the general assumption of similarity between average strains of the reinforcement and concrete. This discrepancy can be attributed to two well-known, but often neglected issues, namely, the effective area of concrete in tension and the end effect [13–16].

The European normative documents [17,18] imply similar expressions for the maximum crack spacing, $s_{r,max}$, assuming it to be a linear combination of two components related to the cover, c , and the ratio of the bar diameter to the reinforcement ratio \varnothing/p :

$$s_{r,max} = k_1 \cdot c + k_2 \cdot \frac{\varnothing}{p}, \quad (1)$$

where k_1 and k_2 are coefficients dependent on various factors (concrete strength, bond quality, loading type, etc.). Considering a simple laboratory tie (square prism with a centre bar), the parameters c , \varnothing , and p become correlated:

$$c = \frac{b-\varnothing}{2} \approx \frac{b}{2}; \quad p = \frac{A_s}{A_c} = \frac{\pi \cdot \varnothing^2 / 4}{b^2 - \pi \cdot \varnothing^2 / 4} \approx \frac{\pi \cdot \varnothing^2 / 4}{b^2}, \quad (2)$$

where b is the side length of square section. Thus, Eq. (1) can be rearranged as

$$s_{r,max} = k_1 \cdot \frac{b-\varnothing}{2} + k_2 \cdot \left(\frac{4b^2}{\pi \cdot \varnothing} - \varnothing \right) \approx k'_1 \cdot b + k'_2 \cdot \frac{b^2}{\varnothing} \quad (3)$$

with coefficients k'_1 and k'_2 , which now include constants $1/2$ and $4/\pi$. This simplification is acceptable if the ratio \varnothing/b is small enough. The common tests, dealing with 100×100 mm cross-section of the prism (i.e. $b = 100$ mm), allow to account only for the effect of the bar diameter. This important limitation should be related to the use of simple specimens in constitutive modelling. The current design approaches, however, were empirically deduced by neglecting that limitation. A number of previous studies, e.g., [19–23], recognised this problem. Moreover, a tie-test typically does not

provide measurements of both, the average deformations of the internal reinforcement bar and the concrete surface. The experimental evidence, however, often contradicts the general assumption of the equivalence of mean strains of the reinforcement and concrete [24].

With an intention to evaluate the effect of reinforcement parameters on cracking and deformations of tensile elements, this paper investigates the behaviour of concrete prisms reinforced with multiple bars. Special equipment has been developed for these tests [25]. The test program consists of 23 ties. The number and diameter of the bars vary from 4 to 16 and from 5 mm to 14 mm, respectively. Two concrete covers are considered as well: the reference 30 mm cover is typical for most structural applications [26], while the alternative 50 mm cover is characteristic of laboratory specimens. The deformation analysis is based on the results obtained by monitoring the average elongations of the reinforcement and the concrete surface. Development of the cracks is investigated using a digital image correlation (DIC) technique. The Model Code 2010 (MC 2010) and Eurocode 2 (EC 2) predictions are compared with the experimental crack distances.

2. Test program

The experimental campaign consists of 23 ties with different arrangement of the reinforcement. Three types of sections (with different reinforcement ratio p) are shown in Fig. 1. As can be observed, each of the groups consists of two or three different reinforcement schemes: 4-bars reference and 16-bars (or 12-bars) alternative. During the previous tests [24,27] it has been shown that the effect of different distribution of bars is most evident in ties with a relatively low reinforcement ratio ($p \approx 1.5\%$). Therefore, two different covers (i.e. 30 mm and 50 mm) are considered in the reference ties with the lowest amount of reinforcement (Fig. 1). Six different bar diameters (Fig. 2) are used.

Gribniak and Rimkus [25] have developed specific equipment for anchorage of multiple bars as shown in Fig. 3. A general aim of the setup is to secure uniform distribution of the applied tension to the bars. The capability to monitor the deformation for each of the bars was another goal of the design. As can be seen in Fig. 3, the anchorage joints embrace two plates connected by a central bar that is connected to the tension device using a spherical hinge. The latter allows reducing a possible imperfection in applying the tensile load. The plates are perforated to fix and distribute the reinforcement bars within the concrete prism. Steel clamps are used for ensuring the confinement of the anchorage joints.

Length of the test specimen (Fig. 3) was limited by capacity of tensile machine. Thus, the length-to-width ratio of the ties was quite low. However, the authors' experience [24,28] indicates that the section area should be related with number of the reinforcement bars. Thus, the 150×150 mm section reinforced with four bars should be split into four segments (each of them associated with a single bar) that doubles of the actual length-to-width ratio. The trial tests [24,27] have also indicated that the cover is very important parameter for ensuring a uniform strain distribution in the concrete: depending on the bar diameter, width of the cross-section reinforced with a single bar should be equal to 60–80 mm. Otherwise, a deformation gradient in concrete, increasing with the cover, makes assumption of the similarity of mean strains of the reinforcement and concrete invalid. The trials also revealed that a relatively short (400–500 mm) concrete prisms with the limited cover might be representative for analysis of the cracking and tension-stiffening effects. The presented test equipment and specimens were designed by accounting the aforementioned conditions.

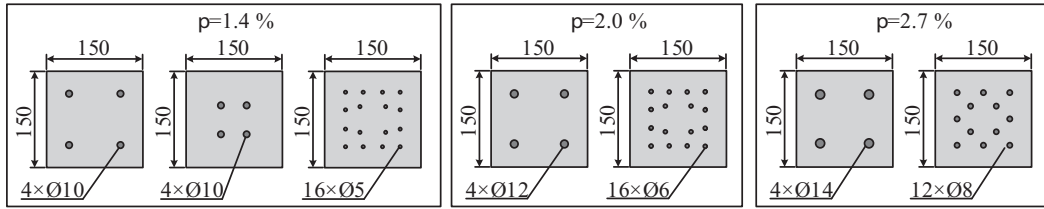


Fig. 1. Cross-sections of the ties (all dimensions in mm).

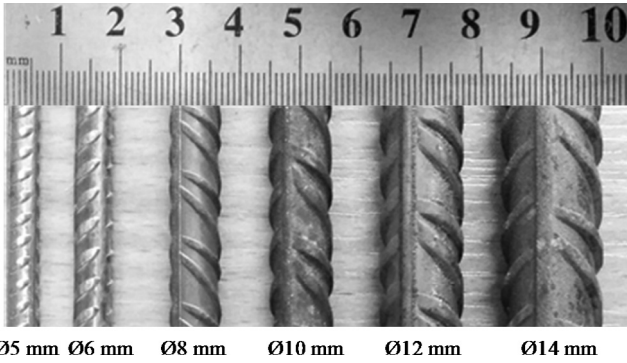


Fig. 2. Reinforcement bars.

2.1. Characteristics of the specimens

Specimens were produced in seven batches using similar concrete mixture with target compressive strength class of C30/37. A site-mixed concrete with a maximum aggregate size of 8 mm was employed. The modulus of elasticity and compressive strength of the concrete were determined using $\varnothing 150 \times 300$ mm cylinders. All samples (including the cylinders) were stored in water to reduce the shrinkage effect. The main characteristics of the specimens are presented in Table 1, where the first two columns refer to the name of the tie and the reinforcement scheme (including the number and diameter of the bars). Other parameters presented in the table are the cover (c), the reinforcement ratio (p), the ratio of the bar diameter to the reinforcement ratio (\varnothing/p), the yield strength (f_y) and modulus of elasticity (E_s) of the bars, the average compressive strength of the concrete on the testing day (f'_{c}) and at 28 days (f_{cm}). The last two columns give the age of the specimen on the testing and the length of the concrete prism (Fig. 3).

2.2. Test results

Initially, the tests were carried out using an electromechanical machine of 100 kN capacity [27]. However, due to the limitation of the maximum load and, most importantly, the length of the concrete prism (≈ 380 mm), the main tests were carried out using a servohydraulic machine of 600 kN capacity under displacement control with 0.2 mm/min loading. The reaction was measured with the electronic load cells of the testing machines. The axial deformations were monitored using linear variable displacement transducers (LVDT), which were attached to the reinforcement bars and to the concrete surface as shown in Fig. 3. The final crack patterns of the ties with the 30 mm cover are shown in Fig. 4, while Fig. 5 presents the cracking schemes of the identical ties with different covers (Fig. 1).

In order to observe the development of the cracks, the front surface of the ties (denoted as “DIC” in Fig. 4) was exposed to a digital image correlation (DIC) system. The cracking schemes were identified using a procedure developed by Rimkus et al. [29]. In Figs. 6 and 7, the cracking schemes obtained by using the relative deformation maps of the surface recognised by the DIC are related to the reference average deformations of the reinforcement measured during the experiments.

Figures 5 and 7 show the cracking schemes of the ties with different cover. The final pattern of the alternative specimens (P8C, P9C) clearly demonstrates the diverse behaviour (length) of the external and internal concrete blocks formed, respectively, between the transverse cracks and at extremities of the prisms. The observed tendencies of the cracking behaviour of the reference ($c = 30$ mm) and the alternative ($c = 50$ mm) ties are also different: slow development of the surface cracks is characteristic of the ties with enlarged cover.

To assess the adequacy of cracking results of the relatively short specimens (380–500 mm), a long 1230 mm tie P5L-4 \times 10 (Table 1) was additionally tested using a lever-arm system developed for

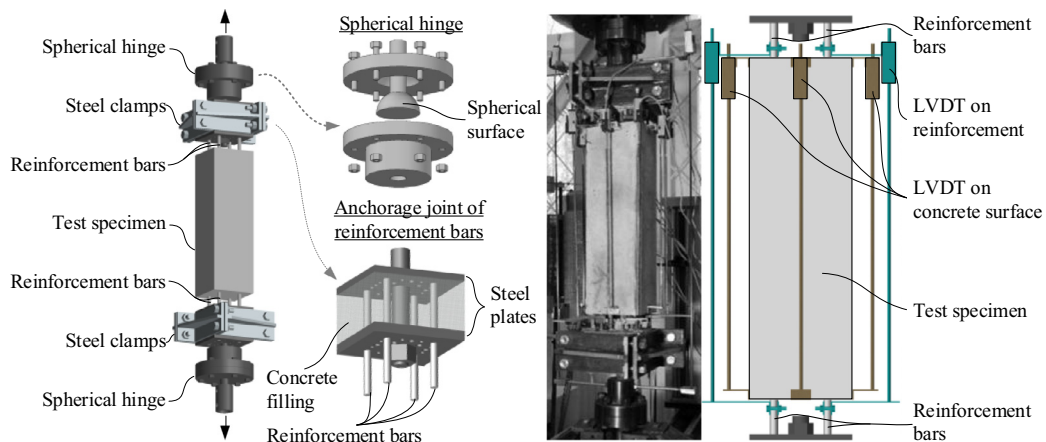


Fig. 3. The test setup of concrete prism reinforced with multiple bars.

Table 1
Main parameters of the ties.

| Tie | Bar properties | c, mm | p, % | \varnothing/p , mm | f_{yt} , MPa | E_s , GPa | f_c , MPa | f_{cm} , MPa | Testing age, days | Specimen length, mm |
|------------|-------------------------|-------|------|----------------------|----------------|-------------|-------------|----------------|-------------------|---------------------|
| P1-4 × 10 | 4 × \varnothing 10 mm | 30 | 1.4 | 714 | 510.1 | 199.5 | 39.5 | 38.6 | 34 | 379 |
| P2-4 × 10 | | 30 | 1.4 | 714 | 510.1 | 199.5 | 41.3 | 39.5 | 41 | 383 |
| P3-4 × 10 | | 30 | 1.4 | 714 | 510.1 | 199.5 | 43.1 | 46.7 | 16 | 503 |
| P4-4 × 10 | | 30 | 1.4 | 714 | 510.1 | 199.5 | 43.1 | 46.7 | 16 | 504 |
| P5-4 × 10 | | 30 | 1.4 | 714 | 510.1 | 199.5 | 40.8 | 44.7 | 15 | 504 |
| P6-4 × 10 | | 30 | 1.4 | 714 | 510.1 | 199.5 | 40.8 | 44.7 | 15 | 496 |
| P7L-4 × 10 | | 30 | 1.4 | 714 | 510.1 | 199.5 | 41.2 | 40.9 | 30 | 1231 |
| P8C-4 × 10 | | 50 | 1.4 | 714 | 510.1 | 199.5 | 40.8 | 45.3 | 14 | 496 |
| P9C-4 × 10 | | 50 | 1.4 | 714 | 510.1 | 199.5 | 40.8 | 45.3 | 14 | 498 |
| P1-16 × 5 | 16 × \varnothing 5 mm | 30 | 1.4 | 357 | 503.9 | 200.7 | 39.5 | 38.6 | 34 | 381 |
| P2-16 × 5 | | 30 | 1.4 | 357 | 503.9 | 200.7 | 41.3 | 39.5 | 41 | 388 |
| P3-16 × 5 | | 30 | 1.4 | 357 | 503.9 | 200.7 | 43.1 | 46.7 | 16 | 503 |
| P4-16 × 5 | | 30 | 1.4 | 357 | 503.9 | 200.7 | 43.1 | 46.7 | 16 | 500 |
| P1-4 × 12 | 4 × \varnothing 12 mm | 30 | 2.0 | 600 | 543.7 | 202.8 | 59.6 | 54.0 | 77 | 503 |
| P2-4 × 12 | | 30 | 2.0 | 600 | 543.7 | 202.8 | 59.6 | 54.0 | 77 | 505 |
| P1-16 × 6 | 16 × \varnothing 6 mm | 30 | 2.0 | 300 | 504.7 | 203.6 | 59.6 | 54.0 | 77 | 493 |
| P2-16 × 6 | | 30 | 2.0 | 300 | 504.7 | 203.6 | 59.6 | 54.0 | 77 | 496 |
| P1-4 × 14 | 4 × \varnothing 14 mm | 30 | 2.7 | 519 | 558.7 | 205.3 | 43.6 | 43.6 | 28 | 494 |
| P2-4 × 14 | | 30 | 2.7 | 519 | 558.7 | 205.3 | 44.0 | 43.5 | 31 | 498 |
| P3-4 × 14 | | 30 | 2.7 | 519 | 558.7 | 205.3 | 44.2 | 43.2 | 34 | 497 |
| P1-12 × 8 | 12 × \varnothing 8 mm | 30 | 2.7 | 296 | 473.9 | 197.1 | 43.6 | 43.6 | 28 | 489 |
| P2-12 × 8 | | 30 | 2.7 | 296 | 473.9 | 197.1 | 44.2 | 43.2 | 34 | 494 |
| P3-12 × 8 | | 30 | 2.7 | 296 | 473.9 | 197.1 | 44.2 | 43.2 | 34 | 499 |

sustained loading cases [30]. Cracking of the long tie was fixed using an optical microscope. In Fig. 8, a final cracking pattern of the long tie P5L-4 × 10 is compared with the cracking maps of the equivalent short ties, which were determined by the DIC system at the same reinforcement deformation level: the comparison is related to the measured average strain $\varepsilon_s = 1.4\%$. The resultant average crack distances of the short and long ties are equal to 100.0 mm and 102.5 mm, respectively.

The average strain diagrams of the reinforcement bars and concrete surface are shown in Figs. 9 and 10, respectively. The differences between the diagrams are evident taking the bare bar response as the reference. The sources of this dissonance are briefly described in the introduction.

3. Discussion of the results

3.1. Cracking behaviour

The different number of cracks is characteristic of the final patterns of the ties reinforced with 4 and 12/16 bars (Fig. 4). However, as shown in Fig. 6, these differences become less significant by comparing the cracking schemes related to the reference deformations of the reinforcement. Figures 5 and 7 show results of the ties with an enlarged cover that is more common for the conventional test samples reinforced with a single bar. The differences in length of the external blocks and the internal segments (between adjacent cracks) are evident. Thus, the mean crack distance assessed by averaging the lengths of all uncracked segments will be inadequate. This problem might be solved by increasing the length of the prism and by excluding the external blocks from consideration. However, uncertainty related to defects of the concrete in the boundary zones would always accompany such a solution [14].

The scatter of individual crack monitoring results obtained using an optical microscope reduces the reliability of the analysis [12]. Therefore, this study considers the cumulative surface displacements as an equivalent of the crack opening. The cumulative deformations were calculated on the base of the relative displacement maps identified by the DIC system (DaVis 8.1.6 software by La Vision) – the position of each point on the surface (digital image) is

identified by applying a particular correlation algorithm to the points from the reference image. The displacement profiles are shown in Fig. 11, where the surface cuts are associated with the position of the reinforcement bars. These profiles were collected from the surface points at every 0.3 mm; the peak displacements correspond to the locations of the actual cracks. The area calculated by integrating the respective profiles represents the cumulative deformation of the surface. For the comparative analysis, it is taken as an equivalent of the total crack opening. The corresponding results of selected ties reinforced with different number of bars are presented in Table 2. It can be observed that the cumulative deformation correlates with number of the bars. The cracking analysis, however, must be related with deformation behaviour of the ties that is evaluated in Section 3.3.

The serviceability analyses described by the Code methods are intended for the stabilized cracking stage [22]. Figure 12 illustrates this issue by relating the cracking schemes (identified by the DIC) to the diagrams of the average bar strains. The strain diagrams also include the stabilized cracking strain limits assessed by the MC 2010. An important observation is that the cracking of the shortest (380 mm) prisms is not stabilized – new cracks were identified by the DIC – though the load-strain diagrams reveal no changes of the stiffness. Alternatively, the cracking of the 500 mm prisms has evidently been stabilized: both the cracking schemes and the average strain diagrams do not demonstrate any changes. The latter characteristic together with the successful results of comparison with the long tie (Fig. 8) enable the 500 mm ties to be used for adequacy verification of approaches adopted in the Design Codes.

The theoretical strain limit associated with beginning of the stabilized cracking stage was assessed by following the MC2010 approach:

$$\varepsilon_{sm} = \sigma_{sr} \frac{1-\beta}{E_s} + \varepsilon_{cm}; \quad \sigma_{sr} = \frac{f_{ctm}}{p} (1 + \alpha_e \cdot p), \quad \varepsilon_{cm} = \beta \frac{f_{ctm}}{E_c}, \quad (4)$$

where ε_{sm} and ε_{cm} are the average strain of reinforcement and concrete, σ_{sr} is the maximum stress in the reinforcement in a crack, β (=0.6) is the coefficient that accounts for type of the loading, f_{ctm} is the tensile strength of the concrete (calculated by MC 2010 using the respective values of the compressive strength and age of the concrete from Table 1), α_e (= E_s/E_c) is the modular ratio; the remaining variable are described in Table 1. Figure 12 clearly

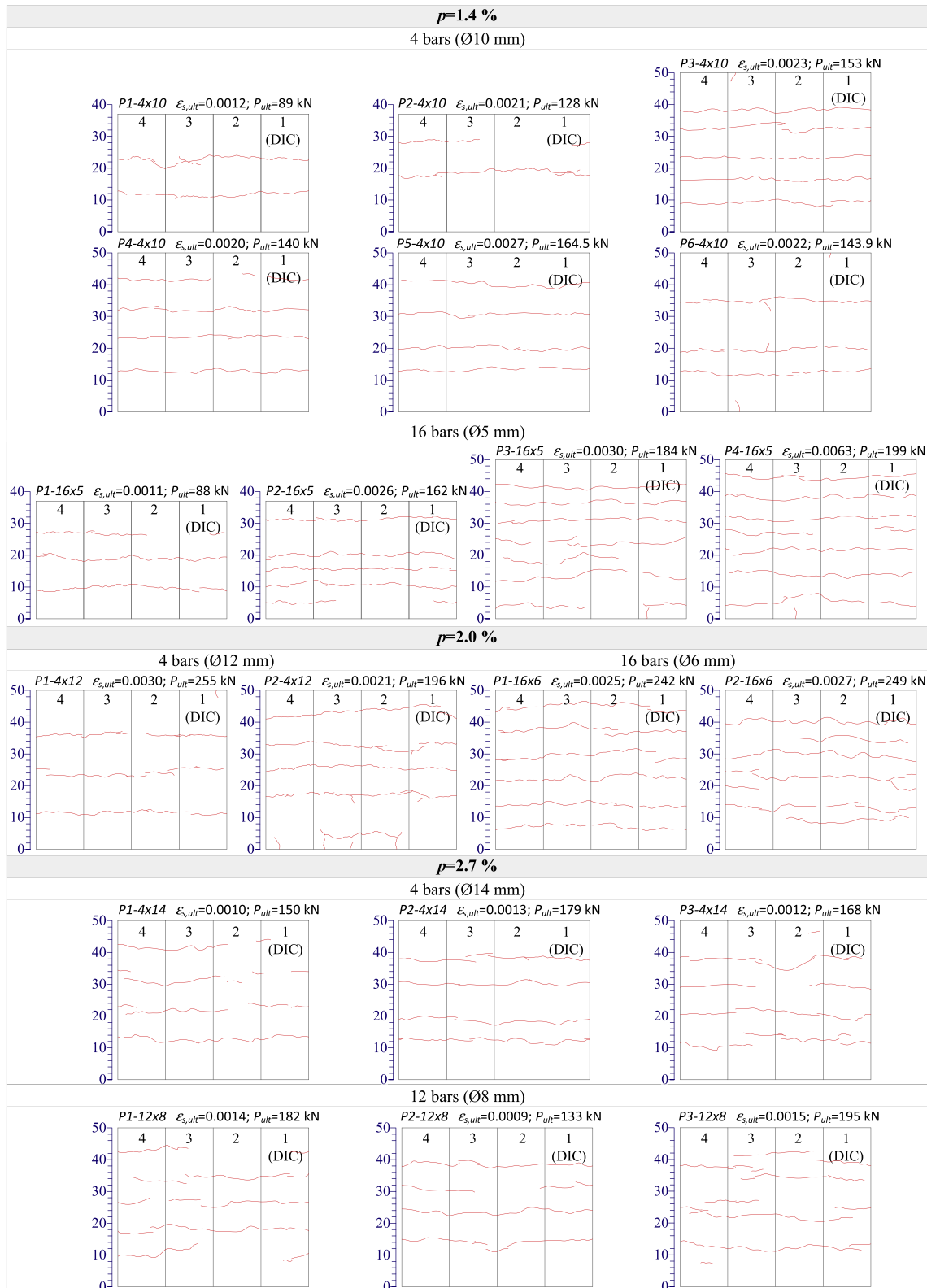


Fig. 4. The final crack pattern of the ties with 30 mm cover.

shows that the strain ϵ_{st} is too radical to identify the stabilized cracking stage if the average deformation of the reinforcement is used as the reference. The opposite results, however, could be obtained in the analysis based on the average deformation of

the concrete surface (Fig. 10). In fact, none of the experimentally observed deformations represents the average deformation behaviour of the tie. The latter can be only approximately assessed with the help of these monitoring results.

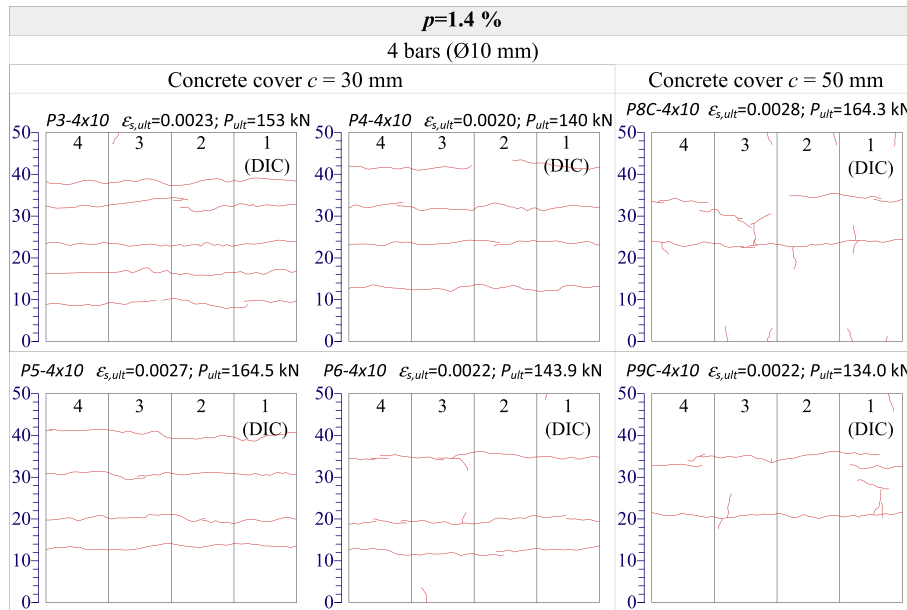


Fig. 5. The final crack pattern of the ties made of the same concrete with different cover.

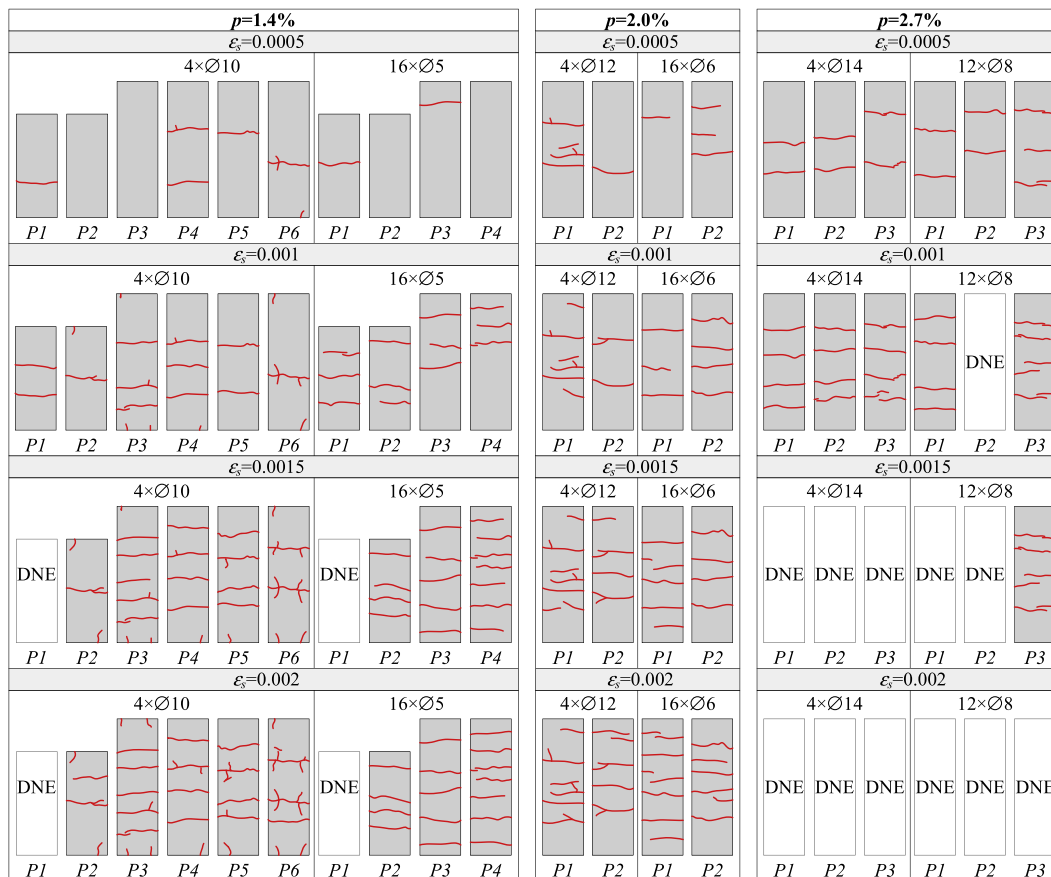


Fig. 6. Crack development identified by the DIC system (the first notation symbols of the ties are presented only; “DNE” = does not exist).

3.2. Verification of the Code predictions

By accounting for the aforementioned inferences, verification of the Design Code predictions is based on the test results of 500 mm ties. Due to a limited number of the measured crack widths, the

verification is limited to the crack spacing. The stabilized cracking stage is associated with the average strain of the reinforcement $\epsilon_s \approx 1.5\text{‰}$ and 1.0‰ for the ties with $p \leq 2.0\%$ and $p = 2.7\%$, respectively. These values are more than three times the cracking limit assessed by Eq. (4). The respective parameters of 15 representative

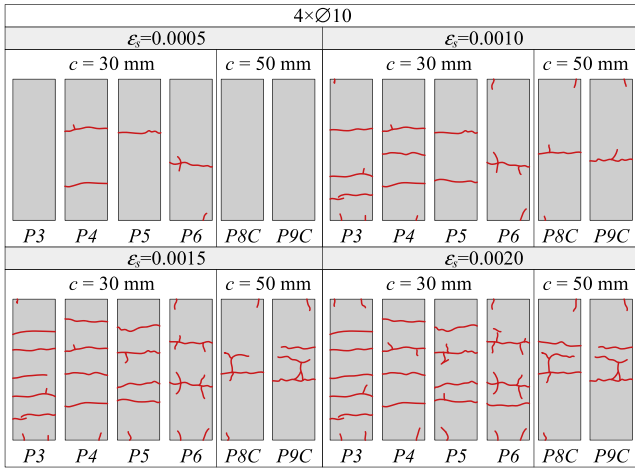


Fig. 7. Crack development identified by the DIC system of ties with different concrete cover ($p = 1.4\%$; the first notation symbols are presented only).

ties (see Fig. 6 for the reference) are given in Table 3. The cracking results (the maximum and average crack distances) of the ties are also presented in Table 3. The maximum spacing was assessed by MC 2010 and EC 2. Two main observations can be made from these results:

1. While the Design Codes predict that maximum crack spacing is dependent on the \varnothing/p ratio, the test results are practically independent on the reinforcement characteristics. As can be observed in Table 3, an increase in \varnothing/p from 300 to 714 causes the corresponding changes of $s_{r,max}$ predicted by the MC 2010 and EC 2 from about 140 mm to 260 mm and from 200 mm to

350 mm, respectively. The test results, however, show the average increase of the maximum distance s_{max} from 100 mm up to 120 mm and the average spacing s_m from almost 90 mm to 100 mm only.

2. The ratio of the experimental maximum-to-average crack spacing (s_{max}/s_m) is practically constant and on average equal to 1.27. Only one tie demonstrates this ratio greater than 1.70 (grey filled cell in Table 3). Such results agree well with the relation identified by Beeby [20]. Fantilli and Chiaia [31] suggested a similar value as a basic parameter for scaling crack patterns.

By investigating structure of the cracking data in Fig. 6 and Table 3, the following aspects are identified. The cracking process of the tie P6-4 × 10 has not evidently been stabilized. A chaotic cracking pattern is characteristic of the tie P1-4 × 12 that has demonstrated an exceptionally high s_{max}/s_m ratio. Consequently, both aforementioned ties were omitted when analysing the cracking tendencies. Fig. 13 relates the maximum distances with the \varnothing/p ratio. The trend line defined using the test data implicitly indicates a tendency different from the Code approaches. Evident overestimation of the crack distances by both Codes are associated to the ties reinforced with four bars: the EC 2 predictions provide more than twofold overestimation, while the MC 2010 demonstrates results that are more accurate. The adequacy of the predictions improves with the decrease of \varnothing/p – the precise predictions by MC 2010 are characteristic of the ties with the minimum \varnothing/p ratio. On the one hand, the observed inaccuracy might be related to the relatively thin (30 mm) cover uncommon to laboratory ties (a square prism reinforced with a centre bar). On the other hand, an important limitation can be related to the application of a simple laboratory tie in the constitutive analysis: refer to the comment on Eq. (3).

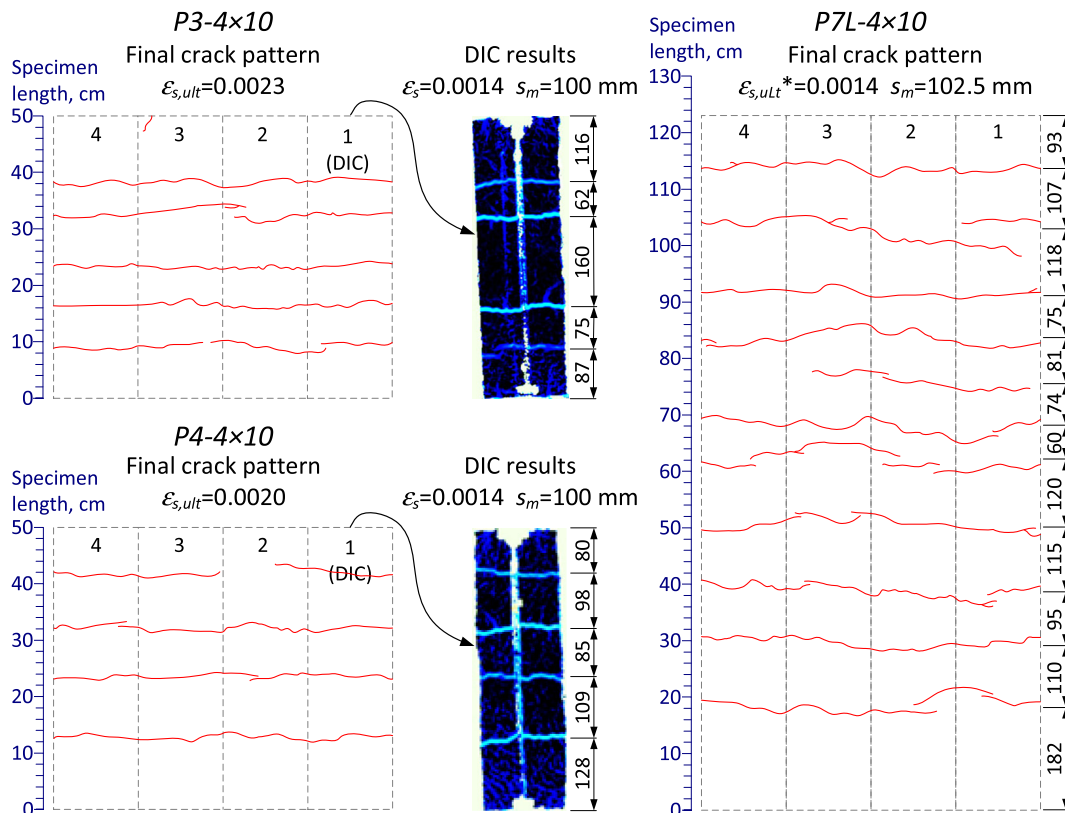


Fig. 8. Cracking results of different length ties (*the maximum deformation allowed by the lever-arm equipment).

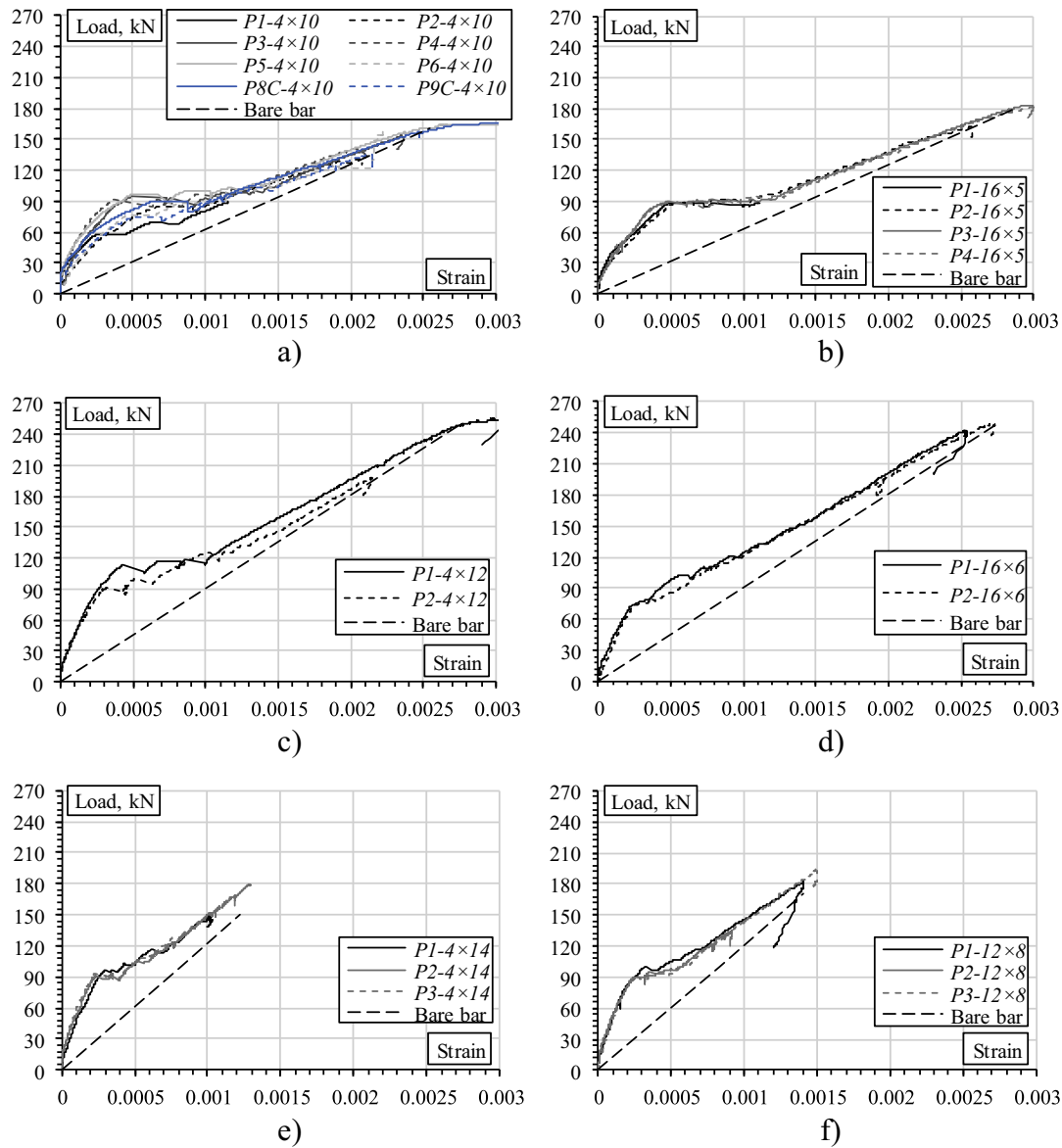


Fig. 9. Average strain diagrams of the reinforcement of the ties with different ratio p : 1.4% (a, b), 2.0% (c, d), and 2.7% (e, f).

Theoretically, the minimum and maximum boundary values of the ratio \varnothing/p considered in Fig. 13 might be represented by the laboratory tie with a 100 mm cross-section reinforced with 32 mm bars ($\varnothing/p = 366$ mm) and 16–18 mm bars ($\varnothing/p = 689$ – 780 mm), respectively. The former specimen has an extremely high reinforcement ratio ($p = 8.75\%$) that is impractical. The latter ties ($p = 2.05$ – 2.61%) are common in testing practice, but the Code predictions demonstrate the particular disagreement with the test results of the ties with the maximum ratio \varnothing/p . Thus, the developed testing setup will be helpful for investigating the effects associated with the variables of Eq. (1). It should be kept in mind, however, that the general idea of the Codes is to formulate a mathematical model (consistent with experimental evidence) that provides a reasonable reliability of the predictions of the maximum crack spacing that can potentially occur. For both standards, the maximum crack spacing refers to a situation in that the crack spacing is equal to twice the transmission length. Since the transmission length was not determined experimentally, the observed results might be considered as a rough approximation to the cracking problem.

3.3. Deformation behaviour

Gribniak et al. [24] related the differences between the diagrams shown in Figs. 9 and 10 to the strain gradient in the concrete by the means of finite element simulation. The strain difference is proportional to the distance between the bars and concrete cover. The mitigation of such differences may reduce the scatter of the deformation responses. This statement is supported by the results presented in Fig. 9a and b and Table 2 that indicate a more uniform distribution of the deformations within the concrete of the ties reinforced with 16 bars. Fig. 14 shows deformation results of the ties considered in Table 2. Although the average strains of the reinforcement are independent on the number of bars (Fig. 14a), noticeable differences of the average strains of reinforcement and concrete surface are evident from Fig. 14b, where the reference deformation levels ($\varepsilon_s = 0.5\text{‰}$ and 2.0‰) correspond to the cracking patterns shown in Fig. 6. The differences decrease with increase of the reinforcement ratio.

Different surface deformations of the concrete at the same strain of the reinforcement indicate the different behaviour of

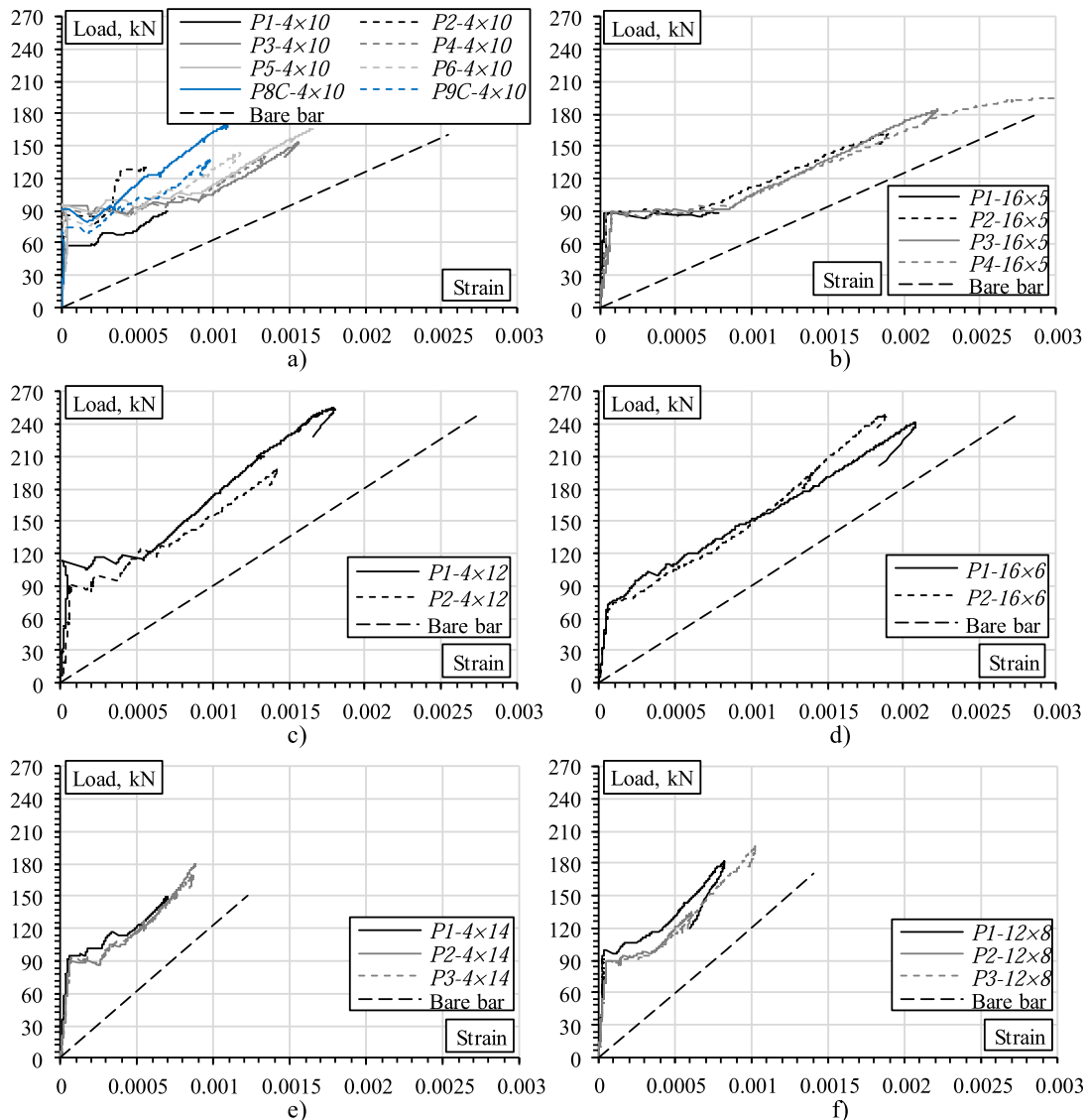


Fig. 10. Average strain diagrams of the concrete surface of the ties with different ratio p : 1.4% (a, b), 2.0% (c, d), and 2.7% (e, f).

the cover that must be accounted for the cracking analysis. Figure 15 presents evidence of the cover effect on the concrete surface deformation of the ties reinforced with four 10 mm bars (Fig. 1). The enlarged cover might stimulate deformations of the concrete surface of opposite magnitude. Such behaviour is characteristic of the tie P8C (Fig. 15), while the similar tie P9C has not accumulated the “negative” strains in consequence of a sudden release of the surface deformations induced by cracking of the concrete. This effect is evident from the zoomed view shown in Fig. 15. These results indicate the importance of the correct evaluation of the strain gradient in the concrete (that might be significant in relatively short ties having a thick cover) for adequate assessment of the structural behaviour of tensile members. This effect is also vital in determining the area of concrete effective in tension and assessing the tension-stiffening effect, i.e. splitting into components related to the contribution of the steel and concrete. Further studies must address the aforementioned problems.

An important observation from Fig. 9 is that the alternative reinforcement distribution schemes are capable at securing practically indistinguishable deformation behaviour of the identical ties, while a significant scatter is characteristic of the reference ties

reinforced with four bars (Fig. 1). Scatter of the results, evident at the early cracking stage in the ties with relatively low reinforcement ratios ($p = 1.4\%$ and 2.0%), could be attributed to the release of fracture energy (during the crack formation) that is more uniform in ties reinforced with 16 bars. Another inference is related to the ties with the enlarged cover, which do not represent any extraordinary deformation behaviour (oppose to the cracking schemes shown in Figs. 5 and 7).

4. Conclusions

A study investigating cracking and deformation behaviour of concrete ties has been carried out. This study is based on test data of 23 concrete prisms reinforced with different number and diameter of the bars. Three section types (with reinforcement ratio equal to 1.4%, 2.0% and 2.7%) are considered. Each of them consists of different reinforcement schemes: 4-bars reference and 16-bars (or 12-bars) alternative. Most of the ties were made with 30 mm cover. To investigate the cover effect, two specimens with the minimum reinforcement ratio were produced with the 50 mm cover.

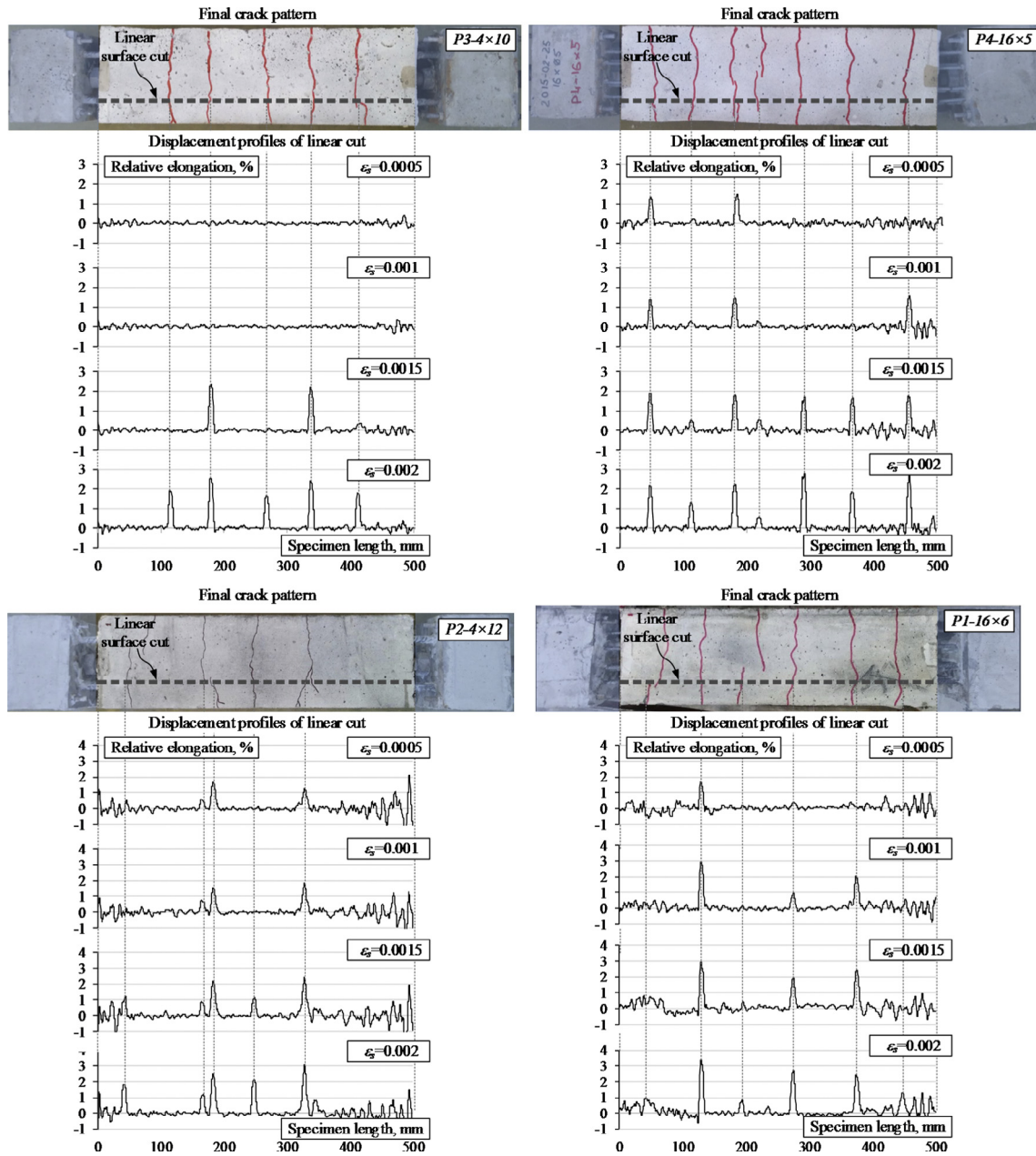


Fig. 11. Distribution of relative displacement of the surface of ties P3-4 × 10 (a), P4-16 × 5 (b), P2-4 × 12 (c) and P1-16 × 6 (d) identified by DIC.

Table 2
Cumulative surface deformations of ties reinforced with different number of bars [mm].

| Tie | p,% | Reference strain of the reinforcement ϵ_s , % | | | |
|-----------|-----|--|------|------|------|
| | | 0.5 | 1.0 | 1.5 | 2.0 |
| P3-4 × 10 | 1.4 | 0.07 | 0.08 | 0.35 | 0.77 |
| P4-16 × 5 | | 0.22 | 0.30 | 0.61 | 0.86 |
| P2-4 × 12 | 2.0 | 0.25 | 0.26 | 0.46 | 0.68 |
| P1-16 × 6 | | 0.40 | 0.67 | 0.86 | 1.17 |

Special equipment has been developed for the tests. Average strains of the reinforcement and concrete surface were used for the deformation analysis. In order to assess the adequacy of the current Design Codes (Model Code 2010 and Eurocode 2), the predicted crack distances were compared to the experimental results. The study reveals that:

1. While the Design Codes predict that maximum crack spacing is dependent on the \varnothing/p ratio, the test results (both maximum and average crack spacings) are practically independent of the reinforcement characteristics. For the limited number of the tested ties, the ratio of the maximum-to-average crack spacing

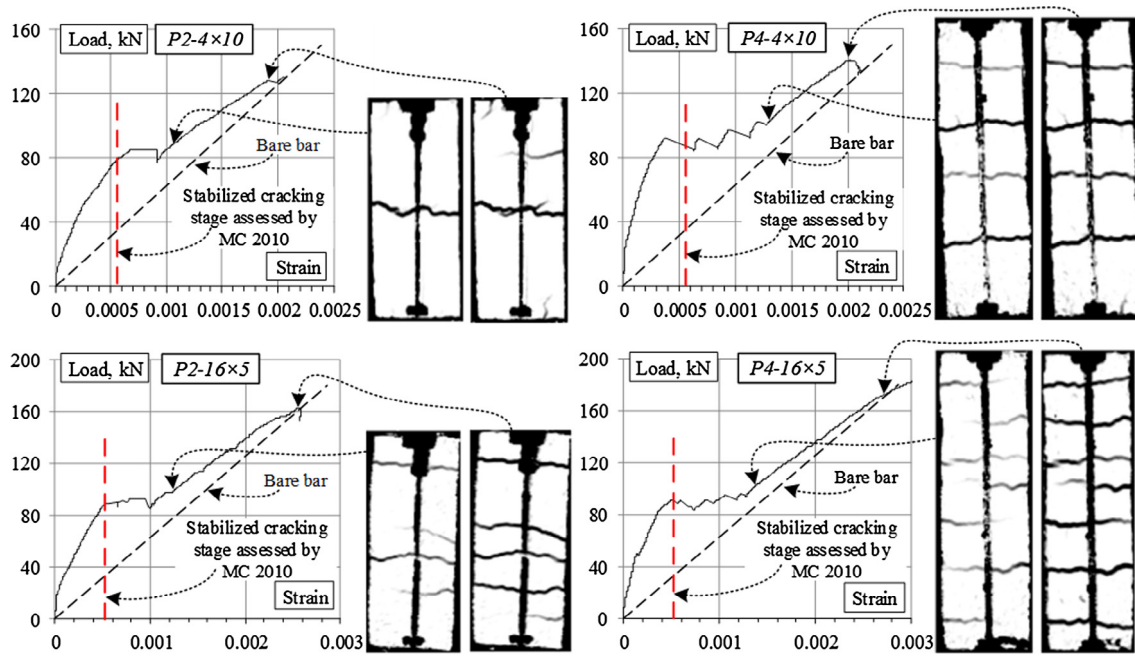


Fig. 12. The location of the stabilized cracking stage.

Table 3
Crack distances sorted by the ratio \varnothing/p .

| Tie | p , % | \varnothing/p , mm | ϵ_{st} , ‰ | Predicted $s_{r,max}$, mm | | Test results | | |
|-----------|---------|----------------------|---------------------|----------------------------|------|----------------|------------|---------------|
| | | | | MC 2010 | EC 2 | s_{max} , mm | s_m , mm | s_{max}/s_m |
| P1-12 × 8 | 2.7 | 296 | 0.283 | 143 | 203 | 170 | 100 | 1.70 |
| P3-12 × 8 | 2.7 | 296 | 0.287 | 143 | 203 | 122 | 100 | 1.22 |
| P1-16 × 6 | 2.0 | 300 | 0.446 | 143 | 203 | 135 | 83 | 1.62 |
| P2-16 × 6 | 2.0 | 300 | 0.446 | 143 | 203 | 130 | 100 | 1.30 |
| P3-16 × 5 | 1.4 | 357 | 0.497 | 159 | 224 | 115 | 83 | 1.38 |
| P4-16 × 5 | 1.4 | 357 | 0.497 | 159 | 224 | 90 | 63 | 1.44 |
| P1-4 × 14 | 2.7 | 519 | 0.275 | 202 | 276 | 127 | 100 | 1.27 |
| P2-4 × 14 | 2.7 | 519 | 0.271 | 202 | 276 | 129 | 100 | 1.29 |
| P3-4 × 14 | 2.7 | 519 | 0.272 | 202 | 276 | 125 | 100 | 1.25 |
| P1-4 × 12 | 2.0 | 600 | 0.447 | 226 | 305 | 130 | 71 | 1.82 |
| P2-4 × 12 | 2.0 | 600 | 0.447 | 226 | 305 | 165 | 100 | 1.65 |
| P3-4 × 10 | 1.4 | 714 | 0.500 | 259 | 346 | 117 | 83 | 1.40 |
| P4-4 × 10 | 1.4 | 714 | 0.500 | 259 | 346 | 125 | 100 | 1.25 |
| P5-4 × 10 | 1.4 | 714 | 0.478 | 259 | 346 | 134 | 100 | 1.34 |
| P6-4 × 10 | 1.4 | 714 | 0.478 | 259 | 346 | 196 | 167 | 1.18 |

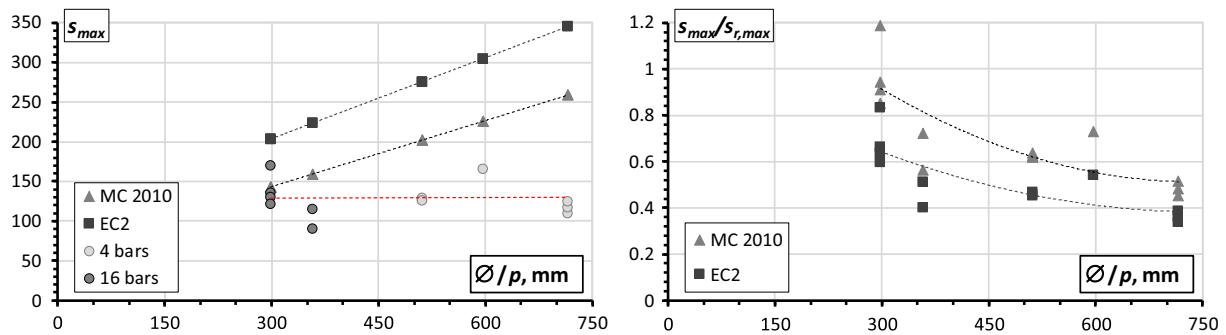


Fig. 13. The effect of \varnothing/p ratio on the maximum crack spacing (left) and the relative predictions (right).

varied between 1.2 and 1.8, on average being 1.27. Only one tie demonstrates a ratio greater than 1.70 that is well agreed with the crack assessment criterion suggested in the literature.

2. At the stabilized cracking stage, predictions of the maximum crack distance were on the safe side. For the reference ties, the Eurocode 2 predictions were overestimated by 120% on

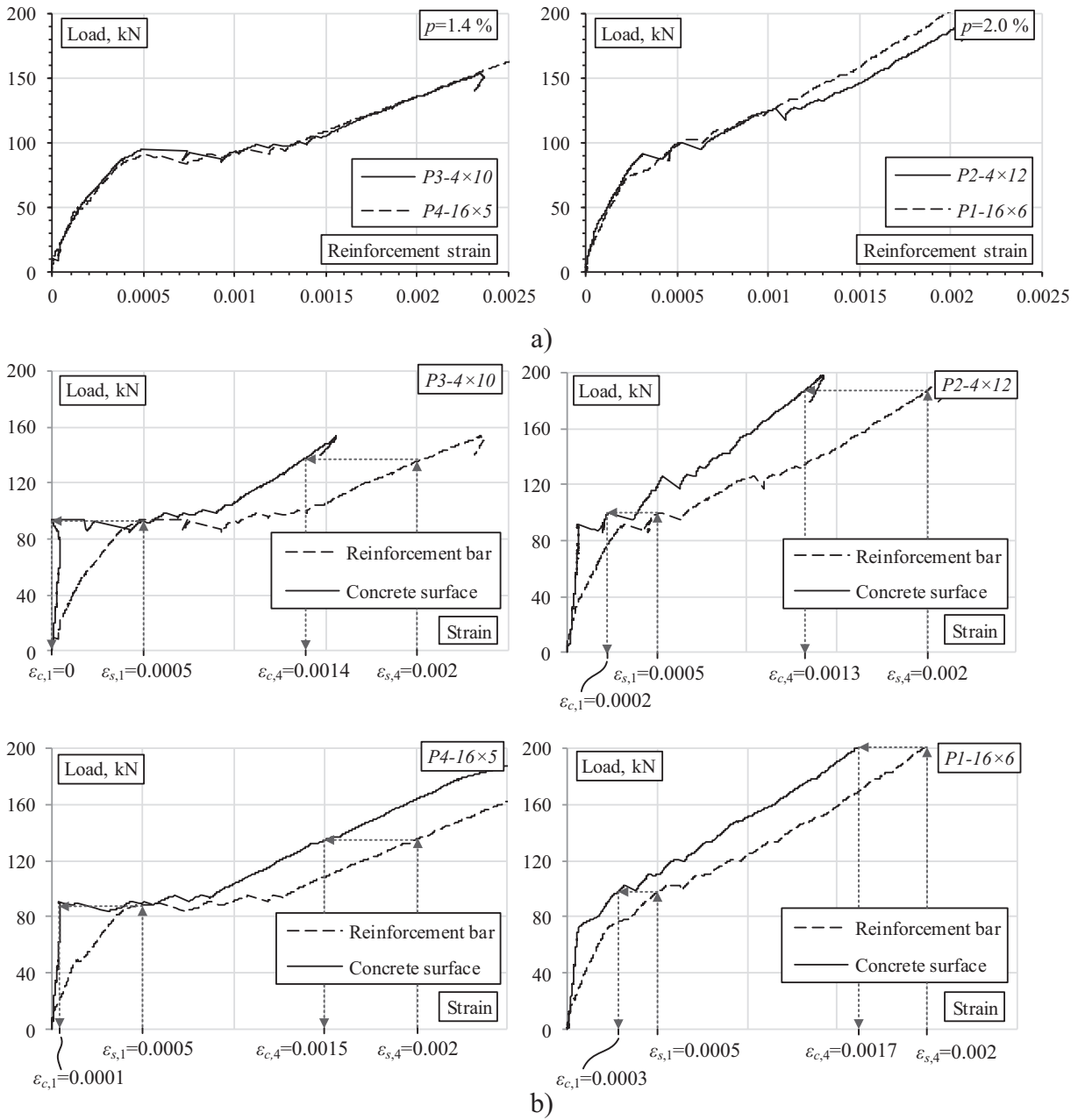


Fig. 14. Average strains diagrams of selected ties: average strains of the reinforcement (a); differences of strains of the concrete surface and reinforcement (b).

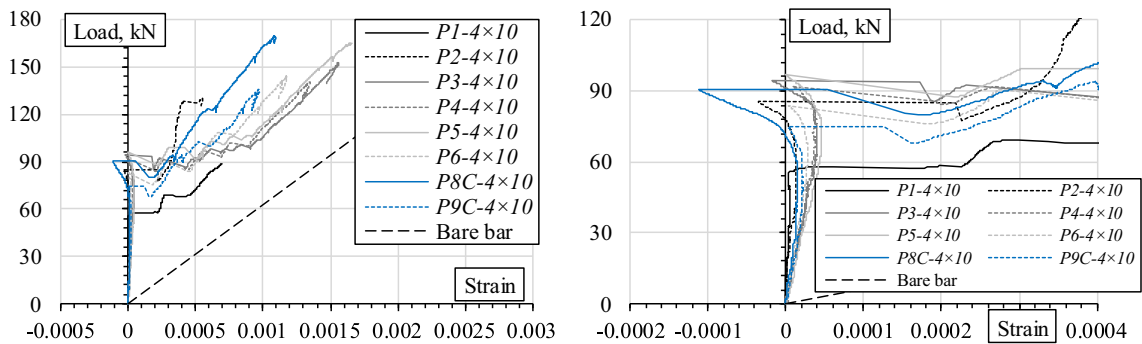


Fig. 15. Average concrete surface strains of the ties with different cover (including zoomed view).

average; the Model Code 2010 demonstrated results that are more precise (with 70% safety on average). The adequacy of the predictions increases with a decrease of the σ/p ratio. For the alternative reinforcement schemes, the respective predictions demonstrated a more rational safety margin, i.e. 80% and 20%. On the one hand, the observed inaccuracy might be related to the relatively thin (30 mm) cover uncommon for laboratory ties (a square prism reinforced with a single bar). On the other hand, an important limitation can be related to application of a laboratory tie in the constitutive analysis: the common tests allow to account only for the effect of the bar diameter.

3. The alternative reinforcement schemes are capable at securing practically indistinguishable deformation behaviour of the identical ties, while a significant scatter is characteristic of the reference ties reinforced with four bars. The scatter is particularly evident at the early cracking stage in the ties with relatively low reinforcement ratios (1.4% and 2.0%). It could be attributed to the release of fracture energy (during the crack formation) that is evidently more uniform in the ties reinforced with 16 bars.
4. Significant differences between the average strains of concrete surface and reinforcement reveal the unreliable character of the deformation assessments based on the surface monitoring results. In the considered case (tension load applied to the bars), the strain gradient is proportional to the distance between the bars and concrete cover. The enlarged cover results in an appearance of “negative” deformations of the concrete surface under the load close to cracking. A reduction of the strain gradient reduces the overall scatter of the deformation response. In the current study, a reduction of the strain gradient was achieved in the ties reinforced with 16 bars. These results indicate the importance of the correct evaluation of the strain gradient (that might be significant in relatively short ties having a thick cover) for adequate assessment of the structural behaviour.

Acknowledgement

The authors gratefully acknowledge the financial support provided by the Research Council of Lithuania (Research Project MIP-050/2014).

References

- [1] F. Rostásy, R. Koch, F. Leonhardt, Zur Mindestbewehrung für Zwang von Außenwänden aus Stahlleichtbeton, Deutscher Ausschuss für Stahlbeton 267 (1976) 1–107 (in German).
- [2] L.S. Hwang, S.H. Rizkalla, Behavior of reinforced concrete in tension at post-cracking range. Engineering Report, Department of Civil Engineering, University of Manitoba, Winnipeg, 1983.
- [3] A. Williams, Test on large reinforced concrete elements subjected to direct tension Technical report 562, Cement and Concrete Association, Wexham Springs, 1986.
- [4] R. Purainer, Last- und Verformungsverhalten von Stahlbetonflächentragwerken unter zweiaxialer Zugbeanspruchung PhD thesis, University of the Federal Armed Forces, Munich, 2005 (in German).
- [5] B.B. Broms, L.A. Lutz, Effects of arrangement of reinforcement on crack width and spacing of reinforced concrete members, ACI J. Proc. 62 (1965) 1395–1410.
- [6] K. Otsuka, Y. Ozaka, Group effects on anchorage strength of deformed bars embedded in massive concrete block, in: Proceedings of the international conference – Bond in concrete from research to practice, Riga, Latvia, 1992, 1, pp. 38–47.
- [7] R. Jakubovskis, G. Kaklauskas, V. Gribniak, A. Weber, M. Juknys, Serviceability analysis of concrete beams with different arrangement of GFRP bars in the tensile zone, ASCE J. Compos. Constr. 18 (2014) 1–10. 04014005.
- [8] E. Gudonis, A. Rimkus, G. Kaklauskas, V. Gribniak, R. Kupliauskas, Experimental investigation on deformation behavior of RC ties, in: Proceedings of the 19th International Conference Mechanika, Kaunas, Technologija, 2014, pp. 94–99.
- [9] V. Gribniak, A.P. Caldentey, G. Kaklauskas, A. Rimkus, A. Sokolov, Effect of arrangement of tensile reinforcement on flexural stiffness and cracking, Eng. Struct. 124 (2016) 418–428.
- [10] A. Borosnyói, I. Snóbli, Crack width variation within the concrete cover of reinforced concrete members, Éptóanyag – J. Silicate Based Compos. Mater. 62 (2010) 70–74.
- [11] A.P. Caldentey, H.C. Peiretti, J.P. Iribarren, A.G. Soto, Cracking of RC members revisited: influence of cover, ϕ/p_{eff} and stirrup spacing – an experimental and theoretical study, Struct. Concr. 14 (2013) 69–78.
- [12] A. Rimkus, R. Jakstaite, R. Kupliauskas, L. Torres, V. Gribniak, Experimental identification of cracking parameters of concrete ties with different reinforcement and testing layouts, Procedia Eng. 172 (2017) 930–936.
- [13] J.P. Forth, A.W. Beeby, Study of composite behavior of reinforcement and concrete in tension, ACI Struct. J. 111 (2014) 397–406.
- [14] R. Tepfers, Cracking of concrete cover along anchored deformed reinforcing bars, Mag. Concr. Res. 31 (1979) 3–12.
- [15] D.H. Jiang, S.P. Shah, A.T. Andonian, Study of the transfer of tensile forces by bond, ACI J. Proc. 81 (1984) 251–259.
- [16] K. Tammo, S. Thelandersson, Crack behaviour near reinforcing bars in concrete structures, ACI Struct. J. 106 (2009) 259–267.
- [17] CEN (Comité Européen de Normalisation), Eurocode 2: Design of Concrete Structures – Part 1: General Rules and Rules for Buildings, EN 1992-1-1:2004, CEN, Brussels, 2004.
- [18] fib (International Federation for Structural Concrete), fib Model Code for concrete structures 2010, Ernst & Sohn, Berlin, 2013.
- [19] L. Elfgren, K. Noghabai, Tension of reinforced concrete prisms. Bond properties of reinforcement bars embedded in concrete tie elements. Summary of a RILEM round-robin investigation arranged by TC 147-FMB “Fracture Mechanics to Anchorage and Bond”, Mater. Struct. 35 (2002) 318–325.
- [20] A.W. Beeby, The influence of the parameter ϕ/p_{eff} on crack widths, Struct. Concr. 5 (2004) 71–83.
- [21] L. Eckfeldt, S. Schröder, Random effects inside the cracking data of RC tests, in: Proceedings of the Sixth International Probabilistic Workshop, Darmstadt, Germany, 2008, pp. 183–205.
- [22] G.L. Balázs, P. Bisch, A. Borosnyói, et al., Design for SLS according to fib Model Code 2010, Struct. Concr. 14 (2013) 99–123.
- [23] P.G. Debernardi, M. Taliano, An improvement of the Eurocode 2 and fib Model Code, methods for the calculation of crack width in RC structures, Struct. Concr. 17 (2016) (2010) 365–376.
- [24] V. Gribniak, A. Rimkus, L. Torres, R. Jakstaite, Deformation analysis of RC ties: Representative geometry, Struct. Concr. (2017), <http://dx.doi.org/10.1002/suco.201600105>.
- [25] V. Gribniak, A. Rimkus, Equipment for fastening group of reinforcement bars within structural concrete element. Patent No. LT 6275 B, State Patent Bureau of the Republic of Lithuania, Vilnius, 2016 (in Lithuanian).
- [26] F. Aslani, S. Nejadi, B. Samali, Instantaneous and time-dependent flexural cracking models of reinforced self-compacting concrete slabs with and without fibres, Computers and Concrete 16 (2015) 223–243.
- [27] A. Rimkus, A. Vilėniškytė, An experimental study of the influence of reinforcement bar arrangement on deformation behaviour and cracking of reinforced concrete members, in: Proceedings of the 18th Conference for Junior Researchers Science – Future of Lithuania, Vilnius, Lithuania, 2015, pp. 1–4 (in Lithuanian).
- [28] V. Gribniak, H.A. Mang, R. Kupliauskas, G. Kaklauskas, Stochastic tension-stiffening approach for the solution of serviceability problems in reinforced concrete: Constitutive modeling, Comput.-Aided Civil Infrastruct. Eng. 30 (2015) 684–702.
- [29] A. Rimkus, A. Podviezko, V. Gribniak, Processing digital images for crack localization in reinforced concrete members, Procedia Eng. 122 (2015) 239–243.
- [30] E. Gudonis, G. Kaklauskas, D. Bacinskas, V. Gribniak, R. Ramanauskas, V. Tamulenas, Experimental investigation on short- and long-term deformations of cracked reinforced concrete ties, in: ASCE Proceedings, CONCREEP 10: Mechanics and physics of creep, shrinkage, and durability of concrete and concrete structures, 2015, pp. 958–962.
- [31] A. Fantilli, B. Chiaia, Golden Ratio in the crack pattern of reinforced concrete structures, ASCE J. Eng. Mech. 139 (2013) 1178–1184.